ACCOUNTS
of chemical research

Carrier Multiplication in Semiconductor Nanocrystals: Influence of Size, Shape, and Composition

LAZARO A. PADILHA,[†] JOHN T. STEWART,[†]
RICHARD L. SANDBERG, WAN KI BAE, WEON-KYU KOH,
JEFFREY M. PIETRYGA, AND VICTOR I. KLIMOV*
*Center for Advanced Solar Photophysics, Los Alamos National Laboratory,
Los Alamos, New Mexico 87545, United States*

RECEIVED ON JULY 31, 2012

CONSPECTUS

During carrier multiplication (CM), also known as multiexciton generation (MEG), absorption of a single photon produces multiple electron–hole pairs, or excitons. This process can appreciably increase the efficiency of photoconversion, which is especially beneficial in photocatalysis and photovoltaics.

This Account reviews recent progress in understanding the CM process in semiconductor nanocrystals (NCs), motivated by the challenge researchers face to quickly identify candidate nanomaterials with enhanced CM. We present a possible solution to this problem by showing that, using measured

biexciton Auger lifetimes and intraband relaxation rates as surrogates for, respectively, CM time constants and non-CM energy-loss rates, we can predict relative changes in CM yields as a function of composition. Indeed, by studying PbS, PbSe, and PbTe NCs of a variety of sizes we determine that the significant difference in CM yields for these compounds comes from the dissimilarities in their non-CM relaxation channels, i.e., the processes that compete with CM. This finding is likely general, as previous observations of a material-independent, "universal" volume-scaling of Auger lifetimes suggest that the timescale of the CM process itself is only weakly affected by NC composition.

We further explore the role of nanostructure shape in the CM process. We observe that a moderate elongation (aspect ratio of 6−7) of PbSe NCs can cause up to an approximately two-fold increase in the multiexciton yield compared to spherical nanoparticles. The increased Auger lifetimes and improved charge transport properties generally associated with elongated nanostructures suggest that lead chalcogenide nanorods are a promising system for testing CM concepts in practical photovoltaics.

Historically, experimental considerations have been an important factor influencing CM studies. To this end, we discuss the role of NC photocharging in CM measurements. Photocharging can distort multiexciton dynamics, leading to erroneous estimations of the CM yield. Here, we show that in addition to distorting time-resolved CM signals, photocharging also creates spectral signatures that mimic CM. This re-emphasizes the importance of a careful analysis of the potential effect of charged species in both optical and photocurrent-based measurements of this process.
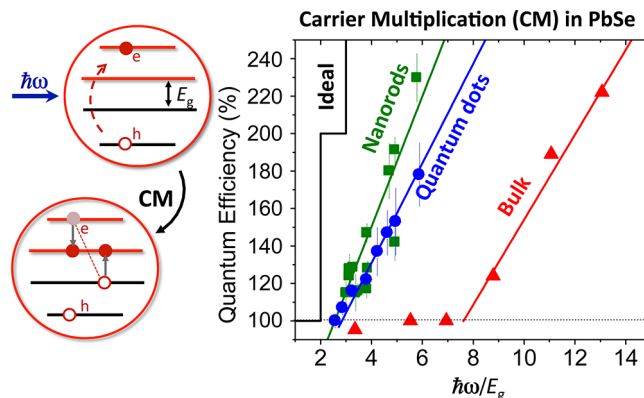
1. Introduction

Carrier multiplication (CM) is a process whereby absorption of a single photon results in multiple electron–hole pairs (excitons). This process could benefit a number of solar-energy conversion technologies, most notably photocatalysis and photovoltaics (PVs).[1,2] For example, a single-junction PV with an ideal CM yield can produce a power

conversion efficiency exceeding 40%,[1,3,4] which is a considerable improvement over the traditional Shockley−Queisser limit of ∼31%.[5] The ideal CM yield is described by a staircase function in which each increment of the incident photon energy ($\hbar\omega$) by the band gap (E_g) results in a new e-h pair, corresponding to an increase of quantum efficiency (QE) of photon to exciton conversion by one or
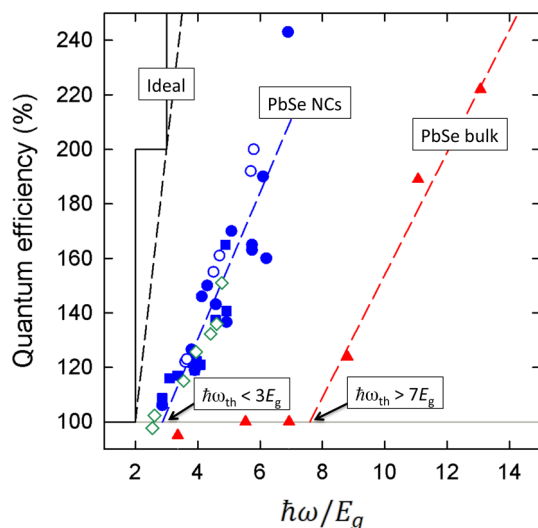
FIGURE 1. CM efficiencies of PbSe NCs (blue and green symbls) and bulk PbSe films (red solid triangle; ref 24) as a function of $\hbar\omega/E_g$. In addition to NC measurements from the present study (blue solid circles and squares), we show results from ref 21 (blue open circles). The CM threshold ($\hbar\omega_{th}$) in NCs is greatly reduced compared to bulk. Note the excellent agreement between transient absorption (blue open circles, blue solid circles), photoluminescence (blue solid squares), and photocurrent (green open diamonds; ref 23) measurements. Ideal cases set by energy conservation are shown by a solid black line (ideal "staircase") and a dashed black line (more realistic dependence with $\varepsilon_{eh} = E_g$).

100% (Figure 1; black solid line). In the CM case, QE is greater than unity and the value of $\eta = (\text{QE} - 1)$ is usually referred to as multiexciton yield.

In bulk semiconductors, CM has been observed since the 1950s and explained by impact ionization. In impact ionization, the collision of a high-energy (hot) conduction-band electron (or valence-band hole) with a valence-band electron promotes it across the energy gap. Two important parameters of this process are the activation threshold ($\hbar\omega_{th}$ in the case of optical excitation) and the e–h pair creation energy (ε_{eh}). The latter is the energy required to generate a new exciton after the CM threshold is reached. In optical measurements, ε_{eh} can be derived from the inverse slope of the dependence of QE on $\hbar\omega$: $\varepsilon_{eh} = [\Delta(\text{QE})/\Delta(\hbar\omega)]^{-1} = [\Delta\eta/\Delta(\hbar\omega)]^{-1}$. Energy conservation dictates that the minimal values of ε_{eh} and $\hbar\omega_{th}$ are E_g and $2E_g$, respectively. However, in bulk semiconductors, because of the additional restrictions imposed by momentum conservation and fast energy losses due to phonon emission, both of these quantities are considerably higher than the ideal, energy-conservation-defined limit. As a result, the benefits of CM in PVs based on traditional bulk solids are negligible.

Quantum-confined semiconductor nanocrystals (NCs), known also as nanocrystal quantum dots, present a promising alternative to bulk materials when it concerns CM. First, a wide separation between NC discrete states has been expected to suppress phonon emission due to a phonon bottleneck[6] and thus favor CM, as was first pointed out by Nozik.[2] Second, three-dimensional (3D) spatial confinement leads to relaxation of translational momentum conservation, which should reduce both $\hbar\omega_{th}$ and ε_{eh}. These considerations motivated a renewed interest in CM with a focus on quantum-confined nanomaterials.

The first experimental observation of CM in quantum dots was reported for PbSe NCs in 2004 by Schaller and Klimov,[7] where CM was detected using the fast Auger decay signatures of multiexcitons[8] in transient absorption (TA). Following this initial report, CM in NCs has become the subject of intense experimental[9−11] and theoretical investigations.[12−15] Early CM studies were mired in confusion, as a large spread in the QEs measured for nominally identical materials appeared in the literature.[16,17] More recent investigations have established that those large discrepancies originated primarily as a result of *extrinsic* factors such as uncontrolled photocharging of NCs.[18−20] After eliminating these artifacts, photocharging-free measurements show good agreement between data obtained by different groups and/or different spectroscopic techniques[19,21,22] (circles and squares in Figure 1). Furthermore, the results of spectroscopic studies of CM have recently been validated by direct photocurrent measurements in photovoltaic devices[23] (diamonds in Figure 1).

2. Carrier Multiplication in Relation to Auger Recombination and Intraband Relaxation

A large body of recent experimental data obtained for PbSe quantum dots indicates that CM efficiency is enhanced compared to bulk PbSe if one accounts for the confinement-induced increase in the band gap energy, which in practice is usually accomplished by analyzing QE as a function of $\hbar\omega/E_g$ (Figure 1). While the use of this approach is still a subject of debate,[16,24] the fact that PbSe NCs are superior to bulk PbSe with regard to energetic output is universally accepted in the community. A further increase of CM yield was observed recently in elongated PbSe nanorods (NRs);[25,26] however, the QEs measured for NCs are still too moderate to significantly improve PV power conversion. In order to achieve a more considerable enhancement in CM, one needs a better understanding of the factors defining ε_{eh} and $\hbar\omega_{th}$.

Initial quantitative insights into CM can be obtained by considering the regime in which a carrier (e.g., an electron) is excited with the energy E_e which is slightly above the CM
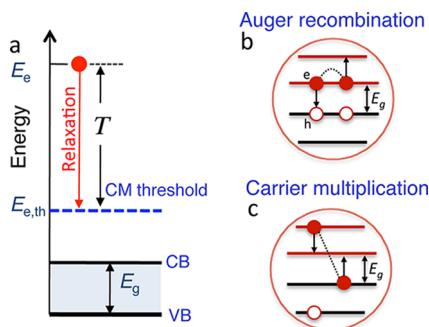
FIGURE 2. (a) The time window available for CM (T) during electron intraband cooling is determined by the excitation energy (E_e), the threshold energy ($E_{e,th}$), and the rate of intraband relaxation; VB and CB are valence and conduction band-edges respectively. (b) In Auger recombination, a biexciton decays to a hot exciton. (c) In CM, which is the inverse of Auger recombination, a hot exciton loses it energy (cools) by promoting a valence-band electron across the band gap.

threshold ($E_{e,th}$) so that the relaxation time window (T) available for CM (Figure 2a) is small compared to the time scale of the individual CM event ($\tau_{e,CM}$). In this case, the probability of generating a new exciton ($p_{e,CM}$) can be estimated from $p_{e,CM} = T/\tau_{CM} = (E_e - E_{e,th})/(k_{cool}\tau_{CM})$, where k_{cool} is the energy-loss rate (measured, e.g., in eV/ps) during intraband cooling due to non-CM processes such as phonon emission. Since photoexcitation produces both an electron and a hole, the total multiexciton yield $\eta = p_{e,CM} + p_{h,CM}$. Assuming that τ_{CM}, k_{cool}, and E_{th} are similar for electrons and holes (lead chalcogenides feature mirror-symmetric conduction and valence bands), we obtain $\eta = (\hbar\omega - \hbar\omega_{th})/(k_{cool}\tau_{CM})$. From $\varepsilon_{eh} = [\Delta\eta/\Delta(\hbar\omega)]^{-1}$, $\varepsilon_{eh} = k_{cool}\tau_{CM}$, which indicates that ε_{eh} is defined by the competition between CM and carrier cooling and suggests that a reduction in ε_{eh} (i.e., increase in QE) can be achieved by reducing k_{cool} and/or τ_{CM}.

Based on these considerations, we can attempt to predict the CM performance of materials based on measurements of k_{cool} and τ_{CM}. However, while k_{cool} can be measured directly by analyzing intraband relaxation,[27] direct measurements of τ_{CM} are not straightforward and have not yet been done. To overcome this problem, we infer the CM time scale from measurements of the inverse process: biexciton Auger recombination (Figure 2b); both are described by the same Coulomb matrix element of the exciton-to-biexciton coupling and are therefore interconnected.

Naively, this reasoning should apply equally well to both bulk and NC semiconductors. However, in the bulk case, the Auger recombination rate (r_A) exhibits an additional exponential thermal activation factor, $\exp(-\zeta E_g/k_B T)$ (T is temperature, k_B is the Boltzmann constant, and ζ is a dimensionless constant), which results from translational

momentum conservation. This factor overshadows the dependence of r_A on the Coulomb matrix element and r_A becomes dominated by a material's band gap energy.[28]

In quantum-confined NCs, relaxation of momentum conservation removes the thermal-activation factor, which leads to E_g-*independent* Auger decay rates.[29] As a result, r_A becomes primarily defined by the Coulomb matrix element and can therefore be directly related to the CM rate. To make this relation more quantitative, we must further consider the involvement of densities of states: single-exciton for Auger decay and biexciton for CM.[30,31] Another important feature of NCs is the universal scaling of Auger lifetimes with the NC volume. This volume-scaling was originally discovered in studies of CdSe NCs[8] and subsequently was observed for many other compositions.[32] Interestingly, not only the size-dependence but also the Auger lifetimes themselves are very similar across different NC compositions including both direct- and indirect-gap materials,[32] despite vastly different Auger constants in their bulk form.[28] While the exact physics underlying these universal trends is not fully understood, it likely relates to the relaxation of momentum conservation, which diminishes the role of the specific band structure in Auger recombination.[32]

The direct relation between CM and Auger decay, together with universal volume-scaling of Auger lifetimes, indicates that CM rates in NCs are also likely to be dominated by NC size and not by composition. This would further suggest that the observed differences in ε_{eh} and QEs for similarly sized NCs of different compositions is mostly due to the differences in intraband cooling rates. To test the validity of this conclusion we have conducted side-by-side studies of NCs of three different lead chalcogenides: PbSe, PbS, and PbTe.

In Figure 3a, we show biexciton Auger lifetimes (τ_{2A}) as a function of confinement energy (E_c): $E_c = E_g - E_{g0}$, where E_{g0} is the bulk energy gap. Consistent with volume scaling, NCs of all three compounds show a similar dependence of Auger lifetime on E_c, which along with similar densities of states, further implies similar τ_{CM} time constants.

In Figure 3b, we show a representative data set which we use to extract the intraband cooling rate near the band edge in PbSe NCs. Specifically, we measure the buildup time (τ_{1P1S}) of the 1S state population by TA and calculate the energy loss rate from the ratio of the 1P-1S energy spacing (ΔE_{1P1S}) and τ_{1P1S}: $k_{1P1S} = \Delta E_{1P1S}/\tau_{1P1S}$.[27] Conducting these measurements for all three materials we find k_{1P1S}(PbTe):k_{1P1S}(PbSe): k_{1P1S}(PbS) $\approx$ 1:2:4. Then, we assume that a similar ratio between cooling rates also holds at energies relevant to CM. Given this comparison of relaxation rates and the similarity in τ_{CM} expected for these three compounds, we would
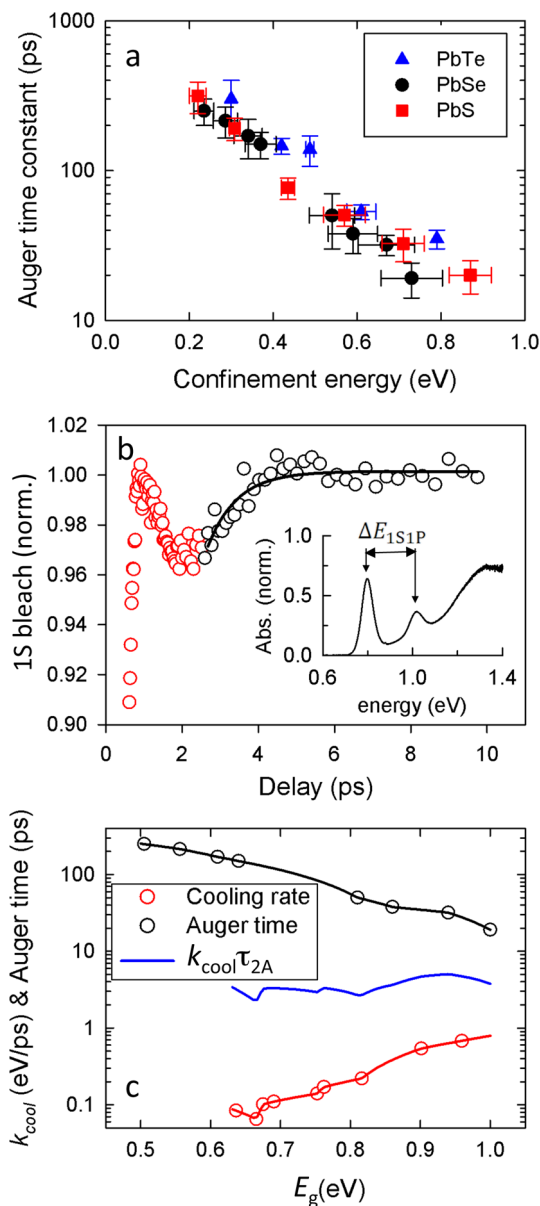
FIGURE 3. (a) Biexciton Auger lifetimes for PbS, PbSe, and PbTe NCs plotted as a function of confinement energy demonstrate a universal trend seen previously for NCs of a variety of compositions. (b) The buildup of 1S bleaching for PbSe NCs measured by TA is used to estimate the intraband cooling rate. The red data points represent the instantaneous Coulomb shift due to hot carriers; it is followed by slower growth due to population transfer from the 1P to the 1S state. The 1S-1P energy separation (ΔE_{1S1P}) is derived from the absorption spectrum (inset). (c) The product of τ_{2A} (black circles) and the cooling rate (red circles) is nearly E_g-independent (blue line) despite strong size dependences that characterize these quantities individually.

expect CM yields to increase going from PbS to PbSe and then to PbTe.

CM measurements shown in Figure 4a as a function of $\hbar\omega/E_g$ (3.1 eV excitation) indeed confirm the predicted trend. CM yields in PbSe NCs are systematically higher than in PbS
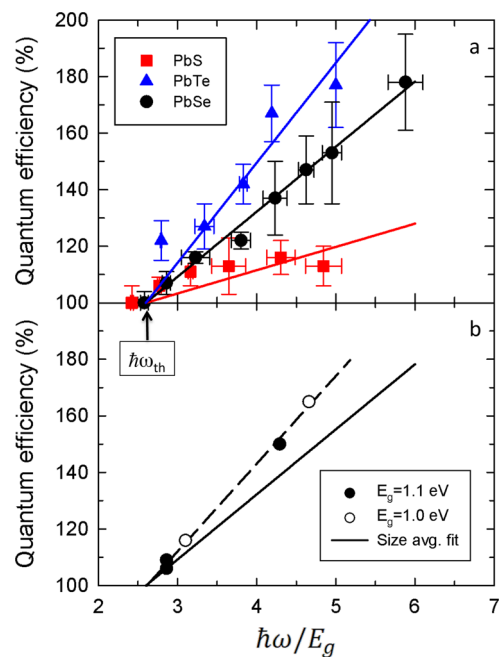

FIGURE 4. Quantum efficiencies (QEs) for PbTe (blue solid triangles), PbSe (●), and PbS (red solid squares) as a function of $\hbar\omega/E_g$ for differently sized NCs; excitation energy is 3.1 eV. (a) Despite their similar Auger time constants (Figure 3a), these materials show strikingly different CM yields, indicative of different e-h pair creation energies. These trends are consistent with the trends in competing cooling rates. (b) The data in (a) provide a size averaged value of ε_{eh} (denoted as $\langle\varepsilon_{eh}\rangle$); solid line. To derive "true" ε_{eh} (dashed line), we conduct measurements for two different excitation energies (3.1 and 4.65 eV) for two PbSe NC samples with similar E_g (1.0 and 1.1 eV; circles), which yields $\varepsilon_{eh} = 3.2E_g$ vs $\langle\varepsilon_{eh}\rangle = 4.3E_g$.

NCs and then further increased in PbTe NCs. For example, for $\hbar\omega = 4.3E_g$, η is 15%, 35%, and 65% in PbS, PbSe, and PbTe NCs, respectively. Importantly, the ratio between these yields (1:2.3:4.3) is close to the relative ratios of the cooling rates (1:2:4).

The CM threshold is estimated by extrapolating the data to $\eta = 0$, which yields ~$2.65E_g$ for all three compositions. This suggests that the observed materials' dependent changes in the CM efficiencies relate primarily to differences in ε_{eh}. Indeed, from the linear fit to the measured data we obtain that ε_{eh} increases from ~$2.8E_g$ in PbTe NCs to ~$4.3E_g$ in PbSe NCs and then to ~$12.5E_g$ in PbS NCs, which is again consistent with expectations based on the analysis of intraband cooling rates. We would like to point out that these determinations of ε_{eh} are size-averaged (denoted below as $\langle\varepsilon_{eh}\rangle$) as they are derived from the QE vs $\hbar\omega/E_g$ measurements for a fixed $\hbar\omega$ and a varied (size-controlled) E_g. In principle, a rigorous determination of ε_{eh} requires the measurements be done on the same sample for a series of different excitation energies. An example of such a measurement is given in Figure 4b, from which $\varepsilon_{eh} = 3.2E_g$. This value

is smaller than $\langle \varepsilon_{eh} \rangle$ ($\sim$4.3E_g), which is likely due to a faster increase of the CM rate with $\hbar\omega$ compared to k_{cool}.

3. The Role of Band Gap Energy in Carrier Multiplication

Throughout this Account, we have consistently expressed ε_{eh} and $\hbar\omega_{th}$ in terms of the band gap energy, E_g. This practice derives from the earliest studies on CM in bulk materials when it was acknowledged that E_g represents the *intrinsic* energy scale in the CM process. Beyond practical considerations, theoretical work for bulk semiconductors has tied ε_{eh} and $\hbar\omega_{th}$ *directly* to E_g by factors of at least 3 and 4, respectively.[33]

As indicated here by the measurements in Figures 1 and 4, NCs also show systematic E_g-dependent trends. This indicates that, as in bulk materials, E_g is an important parameter in the CM process in NCs. Specifically, an almost linear dependence of QE on $\hbar\omega/E_g$ observed in the measurements where the $\hbar\omega/E_g$ ratio is varied by varying the band gap (Figure 4a) suggests that ε_{eh} is directly proportional to E_g: $\varepsilon_{eh} = \beta E_g$, where β is a size-independent constant. This observation, together with a previously derived expression for ε_{eh} ($\varepsilon_{eh} = k_{cool}\, \tau_{CM}$),[34] suggests that the product of k_{cool} and τ_{CM} is proportional to E_g.

To better understand this behavior, we can invoke the known size-dependent trends for the intraband energy loss rate (k_{1P1S}) and Auger recombination (τ_{2A}). Early studies of CdSe NCs indicated that k_{1P1S} scaled as R^{-3} while τ_{2A} approximately as R^{3},[8,35] where R is the NC radius. More recent measurements indicate that similar types of scaling hold also for PbSe NCs[32,36] (see Figure 3c). These observations for strikingly different compounds suggest that the product of k_{1P1S} and τ_{2A} is E_g independent and may itself be another universal trend in NCs. Combining this observation with the previous expression for ε_{eh}, we find $\varepsilon_{eh} = k_{cool}\tau_{CM} = \rho\, k_{1P1S}\, \tau_{2A}$, where ρ is a coefficient which accounts for the effect of densities of exciton and biexciton states. Based on our observation of E_g-independence of $k_{1P1S}\tau_{2A}$ together with direct scaling of ε_{eh} with the band gap energy, we can conclude that ρ is likely linear in E_g.

4. Effect of Nanocrystal Shape

While our previous discussions focused on correlating Auger time constants to CM efficiencies in spherical NCs (zero-dimensional, 0D, materials) and their differences from bulk (3D materials), studies of elongated NRs, which span the 0D and 1D confinement regimes, present an opportunity to fully appreciate the effect of dimensionality on these
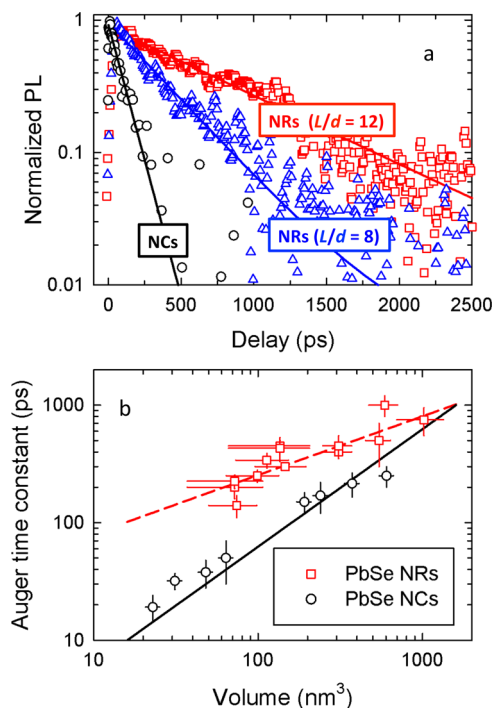

FIGURE 5. (a) Biexciton dynamics for different PbSe NR aspect ratios measured using time-resolved PL; all samples have a similar band gap of $\sim$0.8 eV. (b) NRs (red open squares) appear to demonstrate a systematic scaling of τ_{2A} with volume (dashed line), which however on average is slower (sublinear) than that for spherical NCs (○; solid line shows linear dependence). A fairly large spread in the NR data in this τ_{2A} vs volume representation suggests that a more rigorous description of size-dependent trends in Auger decay in NRs should account separately for changes in their diameter and length.

phenomena. Recent progress in synthesis of high quality PbSe NRs[37] has stimulated active spectroscopic studies aiming to understand the effect of a quasi-1D structure on electronic states, optical spectra,[38] carrier dynamics, and CM in infrared-active nanomaterials.[25,26] The first reports on CM in PbSe NRs[25,26,38] have indicated that elongated NCs exhibit enhanced CM compared to the spherical NCs discussed earlier.

Here, we examine side-by-side CM and Auger recombination in PbSe for both spherical quantum dots and NRs. In Figure 5a, we show the photoluminescence (PL) decay for PbSe NRs of two different aspect ratios ($L/d = 8$ and 12; L is the rod length and d its diameter) and compare to quantum dots; all three samples have similar radii and, hence, similar E_g of $\sim$0.8 eV. The measurements indicate that τ_{2A} is longer in NRs than in spherical nanoparticles and increases with the NR volume (V) following on average a sublinear dependence on V (V changes through both L and d), which is slower that the linear scaling observed for the quantum dots (Figure 5b). Interestingly, as indicated by PbSe NR measurements of ref 38, the dependence of τ_{2A} on L for a fixed d is close to linear.
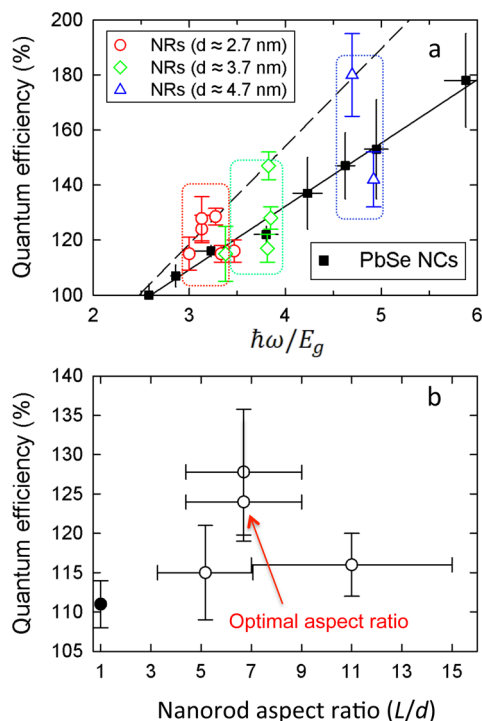
FIGURE 6. CM efficiencies in PbSe NRs vs spherical NCs (quantum dots) at 3.1 eV excitation. (a) NRs with similar diameters (that is, similar E_g) show a large spread for the CM yield, suggesting the influence of aspect ratio (L/d). Based on best QEs in NRs, $\langle \varepsilon_{eh} \rangle$ is $\sim$2.5E_g (dashed line) vs $\sim$4.3E_g in PbSe quantum dots (solid line). (b) A closer look within a subgroup of NRs of similar diameter reveals the importance of aspect ratio.

Given on average a sublinear dependence of τ_{2A} on V, this suggests that the dependence of τ_{2A} on d is likely slower than quadratic.

Based on our discussions above, longer τ_{2A} in NRs seems to be suggestive of a reduced strength of the Coulomb interaction, which should result in reduced CM rates. However, according to CM measurements shown in Figure 6a (excitation at 3.1 eV), NRs are either similar or more efficient than quantum dots and show the overall trend seen in NCs, namely, that the QE increases with increasing $\hbar\omega/E_g$. We see, however, that for a given $\hbar\omega/E_g$ the NR data show a significant spread, indicating that in addition to the NR radius (a primary factor in defining E_g) its length (that is, aspect ratio) is also an important parameter in the CM process. The significant dependence of CM performance on degree of elongation is illustrated in Figure 6b (NR diameters are $\sim$2.7 nm). These data show a progressive increase in multiexciton yield from $\sim$11% in quantum dots to 15% in NRs with the aspect ratio of $\sim$5 and then to $\sim$25% for the aspect ratio of $\sim$7. A further increase in L/d leads to decreasing QE. For example, when L/d increases to 11, η drops to $\sim$15%. Repeating this measurement

for various diameters indicates that the diameter-independent optimal aspect ratio is 6–7. This suggests that NC elongation can produce an approximately 2-fold increase in the CM yield. From the QEs measured for NRs of the optimal ratios, $\langle \varepsilon_{eh} \rangle$ in PbSe NRs is $\sim$2.5E_g (dashed line in Figure 6a) vs $\langle \varepsilon_{eh} \rangle = 4.3E_g$ in PbSe quantum dots (solid line in Figure 6a).

As we established above, it is informative to correlate the increase in CM yields with Auger lifetimes. However, the trend seen for varying aspect ratio is somewhat unexpected. Namely, as the aspect ratio increases and the CM yield goes up, we observe that τ_{2A} increases as well, which seems to be suggestive of *lower* CM rates. To reconcile these apparently contradictory observations, we have to account for the fact that in the elongated structures the character of high-energy excitations involved in CM is different from that of relaxed excitations participating in Auger decay. Specifically, due to the quasi-1D character of NRs, which leads to *enhanced* Coulomb interactions, the relaxed e-h pairs bind into tightly confined 1D excitons.[39] As a result, Auger recombination occurs not as a three-particle collision (as in quantum dots) but as a two-particle, bimolecular interaction between two excitons.[40] Because of charge neutrality of excitons, the rate of Auger decay is expected to be slower than that for unbound e-h pairs. This effect is likely responsible for lower Auger recombination rates in NRs compared to quantum dots (Figure 5b).

The role of excitonic correlations is less significant in CM as this process involves hot unrelaxed charges *before* they form bound states. Therefore, CM in NRs likely occurs in the way similar to that in quantum dots, but via a stronger 1D Coulomb potential.[39] As a result, CM is enhanced in NRs with moderate aspect ratios. The drop in CM efficiency at larger aspect ratios is likely due to restoration of 1D translation momentum conservation which imposes additional restrictions on the CM process.

5. Artifacts in Carrier Multiplication Measurements: Effect of Photocharging

As was mentioned earlier, a significant challenge in initial studies of CM in NCs was a large spread in the measured multiexciton yields due to uncontrolled photocharging.[18−20] In a typical CM experiment, one measures carrier population decay via TA or time-resolved PL under extremely low pump fluence. The development of a fast, subnanosecond Auger decay component at high spectral energies serves as a signature of CM. Further, the amplitude of this component (A) normalized by the height (B) of a slow single-exciton background is used to quantify QE (Figure 7a). In the PL experiment, the A/B ratio can be directly related to the multiexciton yield by $\eta = (A/B - 1)/3$.[18,19]
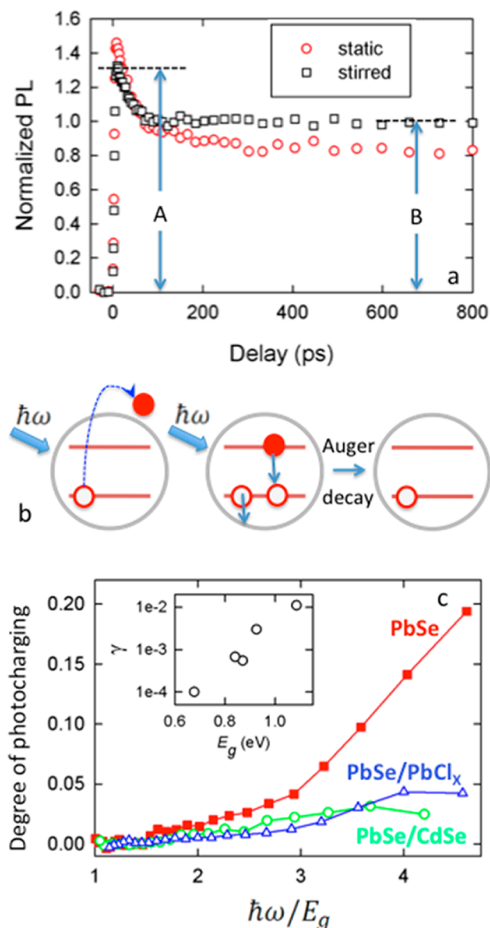
FIGURE 7. (a) Effects of photocharging are revealed when one compares PL dynamics for stirred (black squares) vs static (red circles) samples. (b) Photocharging may lead to false CM-like fast decay signatures due to Auger recombination of charged excitations. (c) In core-only PbSe NCs, the degree of photocharging quickly increases with increasing photon energy (red squares) as expected for hot-carrier trapping; inset shows that the ionization probability (γ) increases with increasing E_g. Photocharging can be suppressed growing an outer shell of CdSe (green circles) or PbCl$_x$ (blue triangles).

In the presence of photocharging, the early time PL signal is increased as the emission rate for charged excitons and multiexcitons is higher than that for their neutral counterparts. On the other hand, the long-time signal is decreased as Auger recombination of charged excitations leaves behind nonemissive uncompensated electrons or holes. As a result, the apparent A/B ratio is increased (Figure 7a), leading to the overestimation of the CM yield. In experimental measurements, the problem of photocharging can be mitigated by stirring[16,18,19,41] or flowing[20] solution samples, which prevents accumulation of charged species in the excitation volume.

A series of recent papers have addressed the mechanism of photocharging in PbSe and PbS NCs.[19,20,41,42] These studies have indicated that this effect is especially pronounced at above band-edge excitation energies and is mediated by hot carrier transfer to trap sites located likely within the ligand shell. The probability of photocharging (γ) is not high ($10^{-4}-10^{-3}$ per absorbed photon);[41,42] however, the lifetime of resulting charge-separated species is extremely long (tens of seconds).[20,41,42] Therefore, even at low-intensity excitation, a large fraction of the NCs in the photo-excited sample can acquire a net charge.

An analysis of the spectral dependence of photocharging in PbS and PbSe NCs indicates a rapid growth of the degree of photocharging (f) with increasing $\hbar\omega$, consistent with a hot-carrier-transfer mechanism for the photoionization process[41,42] (Figure 7c; PbSe NCs). At any given excitation wavelength, the photoionization probability shows significant sample-to-sample variations, likely due to variations in the NC surface/interface properties and/or the composition of the ligand shell. However, using samples with similar surface chemistry, one can resolve certain size-dependent trends. Specifically, the ionization probability typically increases with decreasing NC size (that is, increasing E_g), as illustrated in the inset of Figure 7c, while the lifetime of charge-separated species produced by photoionization decreases.[42]

Since photocharging relies on charge tunneling from the NC to an external trap site, its probability should be reduced if one introduces an external shell of a wider gap material. Indeed, by overcoating a PbSe core with a thin shell of CdSe[42] or PbCl$_x$,[43] one can significantly suppress photocharging (Figure 7c), indicating that these structures can help evaluate true, photocharging-free CM yields of device-grade NC films.

6. Summary

In this Account, we have summarized recent progress in understanding CM and related phenomena in semiconductor NCs. Side-by-side studies of CM, Auger recombination, and intraband relaxation in NCs of PbS, PbSe, and PbTe reveal informative size-, composition-, and shape-dependent trends in these processes. In order to evaluate the relative CM performance of various nanomaterials, we recommend the use of the e-h pair creation energy (ε_{eh}). This quantity captures the competition between the generation of new e-h pairs (time constants τ_{CM}) and energy losses due to intraband relaxation (rate k_{cool}); in the limit of weak CM, $\varepsilon_{eh} = k_{cool}\tau_{CM}$. By using Auger lifetime as a "surrogate" for τ_{CM}, we demonstrate that the difference in the CM yields among quantum dots of PbS, PbSe, and PbTe is mostly due to the difference in the rates of intraband energy losses while the CM rates for these three compositions are likely similar.

One observed trend is direct scaling of ε_{eh} with size-dependent energy gap ($\varepsilon_{eh} \approx \beta E_g$), which is manifested in an approximately linear growth of QE with $\hbar\omega/E_g$. While being functionally similar to the trend observed in bulk semiconductors, in NCs, this seemingly simple scaling arises from a complex interplay between correlated size dependent changes in τ_{CM} and k_{cool}. A strong indication for this yet-to-be-understood correlation is provided by the observation that the product of the Auger lifetime and the 1P-1S energy loss rate ("surrogates" for τ_{CM} and k_{cool}, respectively) is nearly size-independent despite strong size dependences of individual quantities that scale respectively as $\sim R^3$ and $\sim R^{-3}$.

An important current challenge in the CM field is the development of nanostructures with CM performance approaching the ideal, energy-conservation defined limit. To this end, interesting opportunities are associated with the use of elongated NCs or NRs. Our initial measurements of PbSe NRs show that the aspect ratio of $\sim 6-7$ seems to be optimal for CM and allows for an approximately 2-fold increase in the CM yield compared to spherical NCs. Another promising direction is the study of heterostructured NCs that should allow for greater flexibility in controlling the strength of carrier−carrier Coulomb interactions, carrier dynamics, and the band gap energy compared to monocomponent particles. Hybrid structures combining semiconductor NCs with nanoscale metals[44] are also of interest due to the potential effect of surface plasmons on both electron−photon and electron−electron interactions.

BIOGRAPHICAL INFORMATION

Lazaro A. Padilha is a Postdoctoral Research Associate in the Nanotechnology and Advanced Spectroscopy (NanoTech) team, Chemistry Division, Los Alamos National Laboratory (LANL). He received his Ph.D. in Physics (2006) from the State University of Campinas, Brazil. His research is focused on light−matter interactions in nanostructures.

John T. Stewart is a Director's Postdoctoral Fellow in the NanoTech Team. He received B.S. degrees in Physics and Mathematics from Texas A&M University (2004) and a Ph.D. in Physics from the University of Colorado, Boulder (2009). His research centers on novel light−matter interactions.

Richard L. Sandberg is a Technical Staff Member in the Center for Integrated Nanotechnologies, LANL. He received a B.S. in Physics from Brigham Young University (2004) and a Ph.D. in Physics from the University of Colorado, Boulder (2009). His current research interests include coherent X-ray imaging and time-resolved spectroscopy of nanomaterials.

Wan Ki Bae is a Postdoctoral Research Associate in the Nano-Tech team. He received his B.S. (2003), M.S. (2005), and Ph.D. (2009) in Chemical Engineering from Seoul National University, South Korea. His research interests include synthesis and characterization of colloidal nanostructures.

Weon-kyu Koh is a Postdoctoral Research Associate in the NanoTech team. He received his B.S. (2000) and M.S. (2002) in Chemistry from Seoul National University, South Korea and a Ph.D. in Inorganic Chemistry from the University of Pennsylvania (2011). His current research interests include synthesis and charge transport properties of colloidal nanocrystals.

Jeffrey M. Pietryga is a Technical Staff Member in the Nano-Tech team. He received a B.S. in Chemistry from the University of Michigan-Flint (1997) and a Ph.D. in Inorganic Chemistry from the University of Texas, Austin (2002). His current research centers on syntheses and characterization of new infrared-active nanocrystal materials.

Victor I. Klimov is a LANL Fellow, the director of the Center for Advanced Solar Photophysics, and the leader of the NanoTech team. He received his M.S. (1978), Ph.D. (1981), and D.Sc. (1993) degrees from Moscow State University, Russia. His current research interests include photophysics of semiconductor and metal nanostructures and their applications in solar energy conversion.

REFERENCES

1 Werner, J. H.; Kolodinski, S.; Queisser, H. J. Novel optimization principles and efficiency limits for semiconductor solar cells. *Phys. Rev. Lett.* **1994**, *72*, 3851–3854.

2 Nozik, A. J. Quantum dot solar cells. *Phys. E (Amsterdam, Neth.)* **2002**, *14*, 115–120.

3 Hanna, M. C.; Nozik, A. J. Solar conversion efficiency of photovoltaic and photoelectrolysis cells with carrier multiplication absorbers. *J. Appl. Phys.* **2006**, *100*, 1–8.

4 Klimov, V. I. Detailed-balance power conversion limits of nanocrystal-quantum-dot solar cells in the presence of carrier multiplication. *Appl. Phys. Lett.* **2006**, *89*, 123118–123113.

5 Shockley, W.; Queisser, H. J. Detailed balance limit of efficiency of p-n junction solar cells. *J. Appl. Phys.* **1961**, *32*, 510–519.

6 Bockelmann, U.; Bastard, G. Phonon scattering and energy relaxation in two-, one-, and zero-dimensional electron gases. *Phys. Rev. B* **1990**, *42*, 8947–8951.

7 Schaller, R. D.; Klimov, V. I. High efficiency carrier multiplication in PbSe nanocrystals: Implications for solar energy conversion. *Phys. Rev. Lett.* **2004**, *92*, 186601.

8 Klimov, V. I.; Mikhailovsky, A. A.; McBranch, D. W.; Leatherdale, C. A.; Bawendi, M. G. Quantization of multiparticle Auger rates in semiconductor quantum dots. *Science* **2000**, *287*, 1011–1013.

9 Ellingson, R. J.; Beard, M. C.; Johnson, J. C.; Yu, P. R.; Micic, O. I.; Nozik, A. J.; Shabaev, A.; Efros, A. L. Highly efficient multiple exciton generation in colloidal PbSe and PbS quantum dots. *Nano Lett.* **2005**, *5*, 865–871.

10 Trinh, M. T.; Limpens, R.; de Boer, W. D. A. M.; Schins, J. M.; Siebbeles, L. D. A.; Gregorkiewicz, T. Direct generation of multiple excitons in adjacent silicon nanocrystals revealed by induced absorption. *Nat. Photonics* **2012**, *6*, 316–321.

11 Gesuele, F.; Sfeir, M. Y.; Koh, W. K.; Murray, C. B.; Heinz, T. F.; Wong, C. W. Ultrafast supercontinuum spectroscopy of carrier multiplication and biexcitonic effects in excited states of PbS quantum dots. *Nano Lett.* **2012**, *12*, 2658–2664.

12 Rabani, E.; Baer, R. Theory of multiexciton generation in semiconductor nanocrystals. *Chem. Phys. Lett.* **2010**, *496*, 227–235.

13 Allan, G.; Delerue, C. Role of impact ionization in multiple exciton generation in PbSe nanocrystals. *Phys. Rev. B* **2006**, *73*, 205423.

14 Franceschetti, A.; An, J. M.; Zunger, A. Impact ionization can explain carrier multiplication in PbSe quantum dots. *Nano Lett.* **2006**, *6*, 2191–2195.

15 Witzel, W. M.; Shabaev, A.; Hellberg, C. S.; Jacobs, V. L.; Efros, A. L. Quantum simulation of multiple-exciton generation in a nanocrystal by a single photon. *Phys. Rev. Lett.* **2010**, *105*, 137401.

16 Nair, G.; Geyer, S. M.; Chang, L. Y.; Bawendi, M. G. Carrier multiplication yields in PbS and PbSe nanocrystals measured by transient photoluminescence. *Phys. Rev. B* **2008**, *78*, 125325.

17 Trinh, M. T.; Houtepen, A. J.; Schins, J. M.; Hanrath, T.; Piris, J.; Knulst, W.; Goossens, A.; Siebbeles, L. D. A. In spite of recent doubts carrier multiplication does occur in PbSe nanocrystals. *Nano Lett.* **2008**, *8*, 1713–1718.

18 McGuire, J. A.; Joo, J.; Pietryga, J. M.; Schaller, R. D.; Klimov, V. I. New aspects of carrier multiplication in semiconductor nanocrystals. *Acc. Chem. Res.* **2008**, *41*, 1810–1819.

19 McGuire, J. A.; Sykora, M.; Joo, J.; Pietryga, J. M.; Klimov, V. I. Apparent versus true carrier multiplication yields in semiconductor nanocrystals. *Nano Lett.* **2010**, *10*, 2049–2057.

20 Midgett, A. G.; Hillhouse, H. W.; Hughes, B. K.; Nozik, A. J.; Beard, M. C. Flowing versus static conditions for measuring multiple exciton generation in PbSe quantum dots. *J. Phys. Chem. C* **2010**, *114*, 17486–17500.

21 Beard, M. C.; Midgett, A. G.; Hanna, M. C.; Luther, J. M.; Hughes, B. K.; Nozik, A. J. Comparing multiple exciton generation in quantum dots to impact ionization in bulk semiconductors: Implications for enhancement of solar energy conversion. *Nano Lett.* **2010**, *10*, 3019–3027.

22 Beard, M. C. Multiple exciton generation in semiconductor quantum dots. *J. Phys. Chem. Lett.* **2011**, *2*, 1282–1288.

23 Semonin, O. E.; Luther, J. M.; Choi, S.; Chen, H. Y.; Gao, J. B.; Nozik, A. J.; Beard, M. C. Peak external photocurrent quantum efficiency exceeding 100% via MEG in a quantum dot solar cell. *Science* **2011**, *334*, 1530–1533.

24 Pijpers, J. J. H.; Ulbricht, R.; Tielrooij, K. J.; Osherov, A.; Golan, Y.; Delerue, C.; Allan, G.; Bonn, M. Assessment of carrier-multiplication efficiency in bulk PbSe and PbS. *Nat. Phys.* **2009**, *5*, 811–814.

25 Cunningham, P. D.; Boercker, J. E.; Foos, E. E.; Lumb, M. P.; Smith, A. R.; Tischler, J. G.; Melinger, J. S. Enhanced multiple exciton generation in quasi-one-dimensional semiconductors. *Nano Lett.* **2011**, *11*, 3476–3481.

26 Sandberg, R. L.; Padilha, L. A.; Qazilbash, M. M.; Bae, W. K.; Schaller, R. D.; Pietryga, J. M.; Stevens, M. J.; Baek, B.; Nam, S. W.; Klimov, V. I. Multiexciton dynamics in infrared-emitting colloidal nanostructures probed by a superconducting nanowire single photon detector. *ACS Nano* **2012**, *6*, 9532–9540.

27 Klimov, V. I.; McBranch, D. W. Femtosecond 1P-to-1S electron relaxation in strongly confined semiconductor nanocrystals. *Phys. Rev. Lett.* **1998**, *80*, 4028–4031.

28 Haug, A. Band-to-band Auger recombination in semiconductors. *J. Phys. Chem. Solids* **1988**, *49*, 599–605.

29 Pietryga, J. M.; Zhuravlev, K. K.; Whitehead, M.; Klimov, V. I.; Schaller, R. D. Evidence for barrierless Auger recombination in PbSe nanocrystals: A pressure-dependent study of transient optical absorption. *Phys. Rev. Lett.* **2008**, *101*, 217401.

30 Schaller, R. D.; Agranovich, V. M.; Klimov, V. I. High-efficiency carrier multiplication through direct photogeneration of multi-excitons via virtual single-exciton states. *Nat. Phys.* **2005**, *1*, 189–194.

31 Luo, J. W.; Franceschetti, A.; Zunger, A. Carrier multiplication in semiconductor nanocrystals: Theoretical screening of candidate materials based on band-structure effects. *Nano Lett.* **2008**, *8*, 3174–3181.

32 Robel, I.; Gresback, R.; Kortshagen, U.; Schaller, R. D.; Klimov, V. I. Universal size-dependent trend in Auger recombination in direct-gap and indirect-gap semiconductor nanocrystals. *Phys. Rev. Lett.* **2009**, *102*, 177404.

33 Alig, R. C.; Bloom, S. Electron-hole-pair creation energies in semiconductors. *Phys. Rev. Lett.* **1975**, *35*, 1522–1525.

34 Stewart, J. T.; Padilha, L. A.; Qazilbash, M. M.; Pietryga, J. M.; Midgett, A. G.; Luther, J. M.; Beard, M. C.; Nozik, A. J.; Klimov, V. I. Comparison of carrier multiplication yields in PbS and PbSe nanocrystals: The role of competing energy-loss processes. *Nano Lett.* **2012**, *12*, 622–628.

35 Klimov, V. I.; McBranch, D. W.; Leatherdale, C. A.; Bawendi, M. G. Electron and hole relaxation pathways in semiconductor quantum dots. *Phys. Rev. B* **1999**, *60*, 13740–13749.

36 Schaller, R. D.; Pietryga, J. M.; Goupalov, S. V.; Petruska, M. A.; Ivanov, S. A.; Klimov, V. I. Breaking the phonon bottleneck in semiconductor nanocrystals via multiphonon emission induced by intrinsic nonadiabatic interactions. *Phys. Rev. Lett.* **2005**, *95*, 196401.

37 Koh, W.-k.; Bartnik, A. C.; Wise, F. W.; Murray, C. B. Synthesis of Monodisperse PbSe Nanorods: A Case for Oriented Attachment. *J. Am. Chem. Soc.* **2010**, *132*, 3909–3913.

38 Padilha, L. A.; Stewart, J. T.; Sandberg, R. L.; Bae, W.-K.; Koh, W.-K.; Pietryga, J. M.; Klimov, V. I. Aspect ratio dependence of Auger recombination and carrier multiplication in PbSe nanorods. *Nano Lett.* **2013**, *13*, 1092–1099.

39 Bartnik, A. C.; Efros, A. L.; Koh, W. K.; Murray, C. B.; Wise, F. W. Electronic states and optical properties of PbSe nanorods and nanowires. *Phys. Rev. B* **2010**, *82*, 195313.

40 Htoon, H.; Hollingsworth, J. A.; Dickerson, R.; Klimov, V. I. Effect of Zero- to one-dimensional transformation on multiparticle Auger recombination in semiconductor quantum rods. *Phys. Rev. Lett.* **2003**, *91*, 227401.

41 McGuire, J. A.; Sykora, M.; Robel, I.; Padilha, L. A.; Joo, J.; Pietryga, J. M.; Klimov, V. I. Spectroscopic signatures of photocharging due to hot-carrier transfer in solutions of semiconductor nanocrystals under low-intensity ultraviolet excitation. *ACS Nano* **2010**, *4*, 6087–6097.

42 Padilha, L. A.; Robel, I.; Lee, D. C.; Nagpal, P.; Pietryga, J. M.; Klimov, V. I. Spectral dependence of nanocrystal photoionization probability: The role of hot-carrier transfer. *ACS Nano* **2011**, *5*, 5045–5055.

43 Bae, W.-K.; Joo, J.; Padilha, L. A.; Won, J.; Lee, D. C.; Lin, Q.; Koh, W.-k.; Luo, H.; Klimov, V. I.; Pietryga, J. M. Highly effective surface passivation of PbSe quantum dots through reaction with molecular chlorine. *J. Am. Chem. Soc.* **2012**, *134*, 20160–20168.

44 Khanal, B. P.; Pandey, A.; Li, L.; Lin, Q.; Bae, W.-K.; Luo, H.; Klimov, V. I.; Pietryga, J. M. Generalized synthesis of hybrid metal-semiconductor nanostructures tunable from the visible to the infrared. *ACS Nano* **2012**, *6*, 3832–3840.